Approved for public release; distribution is unlimited.

Parametric Study of a Finite Element Model of the Sidewinder Missile

by

Gregory G. Van Dyke

Lieutenent, United States Navy

B. S. Southern Utah State University, 1982

Submitted in partial fulfilment of the requirements for the degree of

MASTER OF SCIENCE IN AERONAUTICAL ENGINEERING

from the

NAVAL POSTGRADUATE SCHOOL
March 1993

ABSTRACT

The long range Maritime Patrol mission has evolved and expanded such that the U. S. Navy's maritime patrol aircraft (P-3C Orion) has become an attractive platform from which to employ a wide variety of air launched weapons. Specifically the need for a stand alone air-to-air defensive capability was identified. In 1989 the Naval Air Test Center at Patuxent River, Maryland began investigation for this through the P-3C/AIM-9 integration program. Naval Postgraduate School responded to this with the construction of a ground vibration test stand and the conduction of a preliminary vibrational characterization of the AIM-9 missile. From these tests a two degree of freedom lumped mass model was developed along with the determination of the primary and secondary missile resonant modes in pitch. In addition, a mathematical model of the AIM-9 missile was developed using finite element techniques. This model was used to analytically determine the modal parameters of the missile and set up a modal test system to experimentally verify the model parameters in view of natural frequencies, mode shapes and transient response. This investigation extends the finite element model utility by refining the model structural code to incorporate an improved mass distribution geometry, thus providing more accurate correspondence between observed natural frequencies and model generated modes and performing a parametric study on the model to discover its sensitivity to conformation and material

REPORT DOCUMENTATION PAGE

Form Approved
OMB No. 0704-0188

1. AGENCY USE ONLY (Leave blank)	2. REPORT DATE	3. REPORT TYPE AND DATES COVERED
	March 1993	Master's Thesis

4. TITLE AND SUBTITLE

Parametric Study of a Finite Element Model of the Sidewinder Missile

5. FUNDING NUMBERS

6. AUTHOR(S)

Gregory G. Van Dyke

7. PERFORMING ORGANIZATION NAME(S) AND ADDRESS(ES)

Naval Postgraduate School
Monterey, CA 93943-5000

8. PERFORMING ORGANIZATION REPORT NUMBER

9. SPONSORING/MONITORING AGENCY NAME(S) AND ADDRESS(ES)

10. SPONSORING/MONITORING AGENCY REPORT NUMBER

11. SUPPLEMENTARY NOTES

The Views expressed in this thesis are those of the author and do not reflect the official policy or position of the Department of Defense or the U.S. Government.

12a. DISTRIBUTION/AVAILABILITY STATEMENT

Approved for public release; distribution is unlimited.

12b. DISTRIBUTION CODE

13. ABSTRACT *(Maximum 200 words)*

The long range Maritime Patrol mission has evolved and expanded such that the U. S. Navy's maritime patrol aircraft (P-3C Orion) has become an attractive platform from which to employ a wide variety of air launched weapons. Specifically the need for a stand alone air-to-air defensive capability was identified. In 1989 the Naval Air Test Center at Patuxent River, Maryland began investigations for this through the P-3C/AIM-9 integration program. Naval Postgraduate School responded to this with the construction of a ground vibration test stand and the conduction of a preliminary vibrational characterization of the AIM-9 missile. From these tests a two degree of freedom lumped mass model was developed along with the determination of the primary and secondary missile resonate modes in pitch. In addition, a mathematical model of the AIM-9 missile was developed using finite element techniques. This model was used to analytically determine the modal parameters of the missile and set up a modal parameters of the missile and set up a model test system to experimentally verify the model parameters in view of natural frequencies, mode shapes and transient response. This investigation extends the finite element model utility by refining the model structural code to incorporate an improved mass distribution geometry, thus providing

14. SUBJECT TERMS	15. NUMBER OF PAGES
Finate Element Analysis, Model Shapes.	59
	16. PRICE CODE

17. SECURITY CLASSIFICATION OF REPORT	18. SECURITY CLASSIFICATION OF THIS PAGE	19. SECURITY CLASSIFICATION OF ABSTRACT	20. LIMITATION OF ABSTRACT
Unclassified	Unclassified	Unclassified	UL

(continued Standard Form 298, Block 13.)

more accurate correspondence between observed natural frequencies and model generated
and performing a parametric study on the model to discover its sensitivity conformatio
material changes. This would anticipate any future missile block upgrades, provide fu
verification of the finite element model and provide model refinement to more accurate
represent the physical structure and behavior. These techniques are inherently missil
generic and could, with proper calibration be applied to any weapon to be loaded on an
platform. This would provide the Navy with an accurate and cost effective methodology
identifying a potential wing flutter problem prior to ever loading and flying a weapon

changes. This would anticipate any future missile block upgrades, provide further verification of the finite element model and provide model refinement to more accurately represent the physical structure and behavior. These techniques are inherently missile generic and could, with proper calibration be applied to any weapon to be loaded on any platform. This would provide the Navy with an accurate and cost effective methodology for identifying a potential wing flutter problem prior to ever loading and flying a weapon.

TABLE of CONTENTS

LIST OF FIGURES

ACKNOWLEDGEMENT

I would like to express my gratitude and appreciation to the following people, without whose support and assistance this work would never have come to fruition.

First to my advisor Dr. Ed Wu. Your expertise, ability, experience and great abundance of "the right stuff" enabled me to complete my course of study. More importantly thank you for the lesson in loyalty and dedication.

Second, to the Departmental Secretary Mrs. Jan Kleinschmidt. Sometimes moral support is the only thing one has, thanks for so much of it.

Finally, my greatest thanks go to my wife Michael, who did the hard things and accomplished impossible tasks. Thank you for keeping everything else running when I couldn't help you. There are many things we didn't get to see or do during our time in Monterey, now maybe we can.

I. INTRODUCTION

A. JUSTIFICATION

As the world political and economic scenes continue to evolve and unfold, several facts seem to surface and resurface in a recurring presentation throughout the theme of this post cold war environment. The first of these is that the United States is the only true superpower remaining on the globe. The great majority of the planet will be looking to us in the years to come for political and economic leadership, technological initiatives as well as world defense and regional security policy. Concomitant with these expectations is the responsibility of the United States to meet these needs. The second fact is that fifty some odd years of the cold war has left the United States on the brink of bankruptcy in an increasingly costly world. With the downfall of the Eastern Bloc nations along with the Soviet Union we find ourselves burdened with supporting a much over-strengthed and vastly miss-apportioned defense structure. Along with this realization has come an increasingly robust military budget reduction and cost saving policy.

Throughout our defense structure we are witnessing a current 25% across the board force reduction which promises to grow to 40 or even 50% as Eastern Europe and the Soviet Union become less and less potent militarily. As our nation presses on into the 1990's we in the Department of Defense are going to be forced to meet our

objectives with less material, a smaller force and with less money. The most expedient way to accomplish these objectives within the above constraints is to expand and utilize our organic resources within the research and development purview, incorporating into these resources, to the maximum extent possible, all available technological advances and analytical aids which will develop the most streamlined and efficient methodologies possible. Once these resources are built, incorporated and utilized, hundreds of projects previously farmed out to defense contractors will be completed reliably, in-house, at a savings of hundreds of millions of dollars.

In this vein this investigation continues the ongoing development of just such an organic resource.

B. BACKGROUND

Since the early to middle 1980's the P-3C Orion has employed to great tactical effectiveness the harpoon anti-ship missile system. However, this weapon addition changed forever the perceived threat potential to opponents as posed by the P3-C. Traditionally the Orion has been utilized and accounted as an open ocean long range anti-submarine platform. It's historical theater of operation has been mid-ocean submarine interdiction, out of the reach of land or sea based air assets. With the development and employment of the sizeable Soviet blue water Navy, as well as the appearance of the many third military threats into the various theaters in which the P3-C is utilized has necessitated the development and incorporation

of an MPA stand alone air-to-air defensive capability. This requirement was registered and quantified at the Naval Air Test Center (NATC) at Patuxent River Naval Air Station under the direction of NavAir. NATC was directed to develop and test an air-to-air defensive combat system incorporating the AIM-9 Sidewinder missile flown and fired from the P3-ORION. This developmental project frontier a quantum leap in mission, tactics and capabilities within the Maritime Patrol community. For the first time the Orion would have the capability to encounter, and with a reasonable chance of success, defeat an air threat. The Harpoon anti-ship mission combined with this new anti-air capability placed the P3-C high on the potential enemies air threat priority.

There are many factors which must be considered when attempting to employ a new weapon system from an established platform. Primary amongst these within the air community is the static and dynamic interaction between the wing and the proposed weapon store. Weapon induced wing flutter is the first and most lethal aerodynamic phenomenon to be addressed.

Every structure or entity that possesses mass and occupies space has as physical characteristics, natural modes and frequencies at which they will vibrate under excitation. When a structure (or conglomerate of structures) is excited at its natural frequency, great increases in vibrational amplitude, leading to structural failure, can occur. Such was the case for the Tacoma Narrows bridge. When excited by a forcing function (in this case the wind) at the spans natural frequency, the vibrational

amplitudes gradually increased until catastrophic failure of the bridge occurred. This case was uniquely noteworthy because the increases in vibrational amplitude occurred over the course of several hours and was well documented. However, the catastrophic failure of an aircraft wing due to flutter induced by exceeding design performance specifications or wing to wing store interaction usually occurs within very few cycles and rarely exceeds more than one or two seconds to failure from onset. Thus the utility and desirability of an accurate flutter prediction methodology is self manifest.

C. PREVIOUS WORK

This thesis is the third in an ongoing investigation to design, build and implement a Navy organic ground vibration test facility and wing flutter prediction methodology.

Initially Lieutenant Commander J. B. Hollyer designed and built a Ground Vibration Test stand (GVT) and utilized it to ascertain experimentally the first three modes in pitch of the AIM-9 Sidewinder missile. From this work a two degree of freedom lumped mass model was developed to represent the missile dynamics. Utilizing Lagrange's equations the following is presented in review for the lumped mass model. Figure 1 presents the spatial geometry, the coordinate systems used and the component make-up of the lumped mass model. Figure 2 depicts the various coordinate assignments used. This is followed by the assumptions made for the theory and organizational definitions for both the mass energy equations and

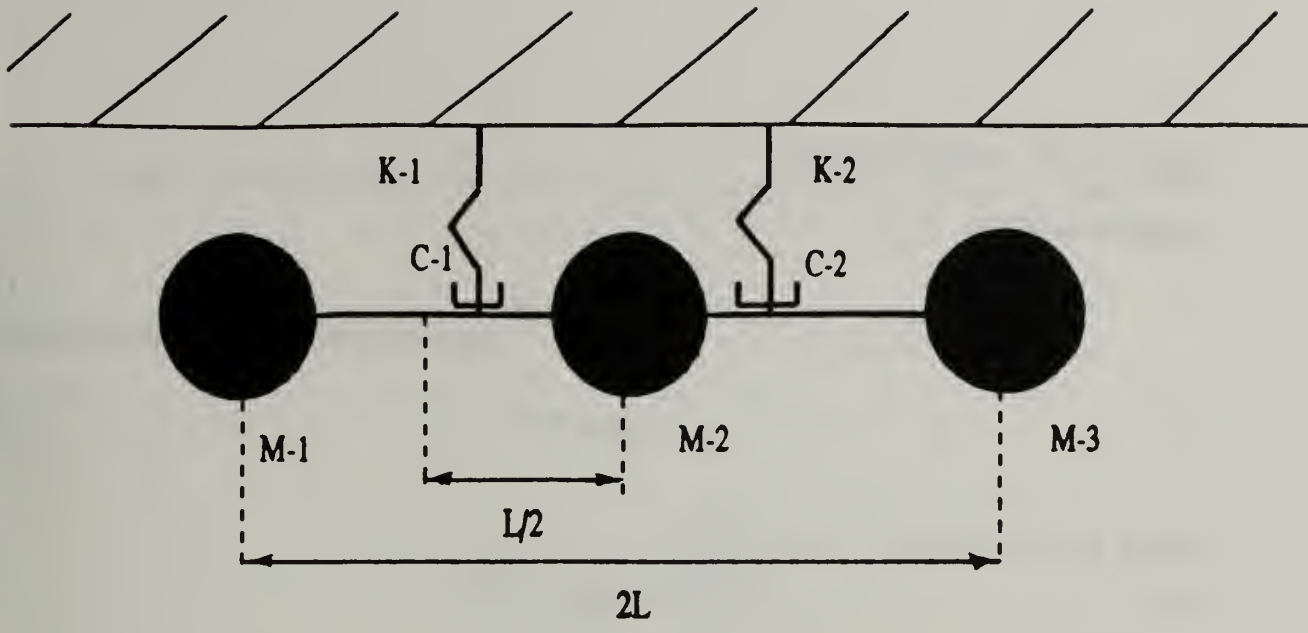

Mass Spring Damper System

Fig. 1

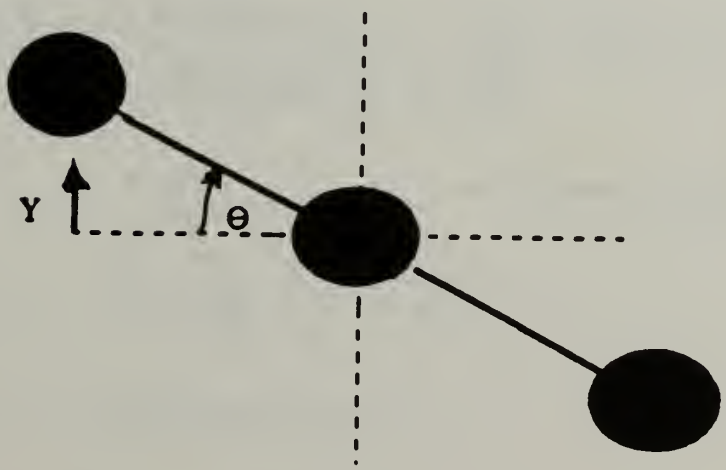

Coordinate System

Fig. 2

the State Space format.

Assumptions:

$$Sin\ \Theta = \Theta \tag{1}$$

$$Cos\ \Theta = 1 \tag{2}$$

Mass connections are rigid:

$$M_1 = M_2 = M_3 = M$$

$$K_1 = K_2 = K$$

$$C_1 = C_2 = C$$

Definitions:

$$Y_1 = Y + L*\Theta \tag{3}$$

$$Y_2 = Y \tag{4}$$

$$Y_3 = Y - L*\Theta \tag{5}$$

T_1 = Kinetic Energy$_1$ = $$1/2 * M_1 * \left(\frac{dY_1}{dt}\right)^2 \tag{6}$$

$$T_2 = 1/2 * M_2 * \left(\frac{dY_2}{dt}\right)^2 \tag{7}$$

$$T_3 = 1/2 * M_3 * \left(\frac{dY_3}{dt}\right)^2 \tag{8}$$

V = Potential Energy =

$$M_1*g*Y_1+M_2*g*Y_2+M_3*g*Y_3+1/2*K_1*(x+L/2*\Theta)^2+1/2*K_2*(x-l/2*\Theta)^2 \quad (9)$$

Using Lagrangian Equations:

$$L'=T-V \quad (10)$$

$$\frac{d}{dt}\left(\frac{\partial L'}{\partial \frac{dq_i}{dt}}\right)-\frac{\partial L'}{\partial q_i}=Q_i \quad (11)$$

$$T=1/2*\left(M_1*\left(\frac{dY}{dt}+L*d\frac{\Theta}{dt}\right)^2+M_2*\left(\frac{dY}{dt}\right)^2+M_3*\left(\frac{dY}{dt}-L*d\frac{\Theta}{dt}\right)^2\right) \quad (12)$$

q_1 @ Y:

$$\frac{\partial L'}{\partial dq_1}=1/2*\left(M*\left(2*\left(\frac{dY}{dt}+L*d\frac{\Theta}{dt}\right)+2*M*\frac{dY}{dt}+2*M*\left(\frac{dY}{dt}-L*d\frac{\Theta}{dt}\right)\right)\right)=M*\left(\frac{dY}{dt}+L*d\frac{\Theta}{dt}\right)+M*\frac{dY}{dt}+M*\left(\frac{dy}{dt}-L*d\frac{\Theta}{dt}\right) \quad (13)$$

$$\frac{d}{dt}\frac{\partial L}{\partial\left(\frac{dq}{dt}\right)}=3*M*d^2\frac{Y}{dt^2} \quad (14)$$

q_2 @ Θ:

$$\frac{\partial L'}{\partial\left(\frac{dq_2}{dt}\right)}=M*L*\left(\frac{dY}{dt}+L*\frac{d\Theta}{dt}\right)+M*L*\left(\frac{dY}{dt}-L*\frac{d\Theta}{dt}\right)=(2*M)*L*\frac{dY}{dt} \quad (15)$$

$$\frac{d}{dt}\left(\frac{\partial L'}{\partial\left(\frac{dq_2}{dt}\right)}\right)=2*M*L*\left(\frac{d^2Y}{dt^2}\right) \tag{16}$$

V = Potential Energy=

$$M*g*(Y+L*\theta)+M*g*Y+M*g*(Y_L*\theta+1/2*K_1*(Y+L/2*\theta)^2+1/2*K_2*(Y-L/2*\theta)^2 \tag{17}$$

q_1 @ Y:

$$\frac{\partial V}{\partial q_1}=3*M*g+K*\left(Y+\frac{L}{2}*\Theta\right)+K*\left(Y-\frac{L}{2}*\Theta\right) \tag{18}$$

q_2 @ Θ:

$$\frac{\partial V}{\partial q_2}=K_1*\frac{L}{2}*\left(Y+\frac{L}{2}*\Theta\right)-K_2*\frac{L}{2}*\left(Y-\frac{L}{2}*\Theta\right) \tag{19}$$

Q_{1*}:

$$3*M*\frac{d^2Y}{dt^2}+(M_1-M_3)*L*\frac{d^2\Theta}{dt^2}+2*K*Y+(K_1-K_2)*L\Theta+3*M*g=F_1 \tag{20}$$

Q_{2*}:

$$2*M*L*\frac{d^2Y}{dt^2}+(M_1-M_2)*L^2*\frac{d^2\Theta}{dt^2}+(K_1+K_2)*\frac{L}{2}*Y+(K_1-K_2)*\frac{L^2}{4}*\Theta+(M_1-M_3)*g*L=F_2 \tag{21}$$

*

$$3*M*\frac{d^2Y}{dt^2}+^{1,3}(K_1+K_2)*Y=F_1 \tag{22}$$

#

$$2*M*L*\frac{d^2Y}{dt^2}+^{2,4}2*K*\frac{L}{2}*Y \tag{23}$$

$$\begin{aligned} 1&=(C_1+C_2)*\frac{dy}{dt} \\ 2&=(C_1+C_2)*\frac{L}{2}*\frac{dy}{dt} \\ 3&=(C_1-C_2)*\frac{L}{2}*d\frac{\Theta}{dt} \\ 4&=(C_1-C_2)*\frac{L^2}{4}*d\frac{\Theta}{dt} \end{aligned} \tag{24}$$

Dropping the last term on the left sides of Equations 23 and 22 due to unnecessary initial conditions and proceeding into the state space format yields:

$Y=X_1$ $\Theta=X_3$

$dY/dt=X_2$ $d\Theta/dt=X_4$

$dX_1/dt=$ X_2

$dX_3/dt=$ X_4

$$X = [X_1\ X_2\ X_3\ X_4]^T \tag{25}$$

$$3*M*\frac{dX_2}{dt}=-2*K*X_1-(C_1+C_2)*X_2-(C_1-C_2)*X_4 \tag{26}$$

$$2*M*L*\frac{dX_2}{dt}=-2*K*\frac{L}{2}*X_1-(C_1+C_2)*\frac{L}{2}*X_2-(C_1-C_2)*\frac{L^2}{4}*X_4 \tag{27}$$

$$I_n = \begin{bmatrix} 1 & 0 & 0 & 0 \\ 0 & (M_1 = M_2 + M_3) & 0 & (M_1 - M_2) * L \\ 0 & 0 & 1 & 0 \\ 0 & (M_1 + M_3) * L & 0 & (M_1 - M_3) * L^2 \end{bmatrix} \quad (28)$$

$$A_n = \begin{bmatrix} 0 & 1 & 0 & 0 \\ -(K_1 - K_2) & -(C_1 + C_2) & -(K_1 - K_2) * \frac{L}{2} & -(C_1 - C_2) \\ 0 & 0 & 0 & 1 \\ -(K_1 + K_2) * \frac{L}{2} & -(C_1 + C_2) & -(K_1 - K_2) * \frac{L^2}{4} & -(C_1 - C_2) * \frac{L^2}{4} \end{bmatrix} \quad (29)$$

The homogeneous problem, representing a system response to an initial condition is:

$$I_n * \frac{dX}{dt} = A_n * X \quad (30)$$

Premultiply by $[I_n]^{-1}$ to obtain:

$$\frac{dX}{dt} = I_n^{-1} * A_n * X \quad (31)$$

The eigenvalue problem can be formed as:

$$[\ \lambda * I - A\ ] * X = [0] \quad (32)$$

For a non-trivial solution, one obtains the charachteristic equation

$$|\lambda * I - A| = 0 \quad (33)$$

Once the eigenvalues, λ_i (i=1 to n) has been found, the mode shapes may be identified using the relation that:

$$\lambda_i * X^{(i)} = A * X^{(i)} \tag{34}$$

where $X^{(i)}$ is the state vector corresponding to the i^{th} eigenvalue λ_i.

$$X(t) = e^{A*t} * X(0) \tag{35}$$

provides the solution for

$$\frac{dX}{dt} = A*X + B*u_{(t)} \tag{36}$$

After the construction of the GVT and the determination of the principal modes in pitch by Lcdr. Hollyer, finite element techniques were used by Mr. Michael Shutty to construct an initial finite element model of the AIM-9 Sidewinder. Utilizing this prototype model Mr. Shutty developed a methodology for utilizing and exploring the various applications of the PAL-2 software used to construct the finite element model.

D. PURPOSE

The purpose of this thesis was to further the development of an existing but incomplete methodology for a Navy organic ground vibrational test and prediction capability. In order to accomplish this, integration of prior work by Lcdr Hollyer and Mr. Shutty was utilized within the framework of this investigation.

E. SCOPE

The evaluation includes refinement and reintegration of the AIM-9 finite element model. This incorporates novel mass location and distribution logic as well as real material characteristics reflecting accurate representation of missile construction. This logic was honed to most accurately represent the missile in terms of modal shapes and frequencies as determined experimentally. A parameterization of missile model properties was then conducted to determine the models sensitivity to geometric as well as material changes.

The parameterization primarily focused on missile component mass and modulus of elasticity changes as well as the replacement of selected structures with potential future improvements in terms of material characteristics.

II. INVESTIGATION

A. GENERAL

Finite element analysis (FEA) is the prediction of structural modes and frequencies utilizing a finite element model to undergo computer generated excitation. A finite element model is the representation of a continuous structure by a discrete one. In the finite element method structures are descretized in that they are represented by discrete grid or node points connected by structural elements. This representation is in the form of a mathematical model consisting of discrete elements connecting discrete node points. The rule of thumb applied to discretization and thus to FEA is that the more node points used the more accurate the solution that is obtained. Also known is that the fewer the nodes the stiffer the model. Unfortunately, for every node point incorporated into the model six degrees of freedom are introduced into the computational analysis. This rapidly becomes the limiting factor in terms of computing time and space as the coefficient matrices become unwieldy.

B. FINITE ELEMENT MODEL

The refined MSC/PAL2 software code developed for this investigation of the AIM-9 Sidewinder geometry is presented in Appendix A. As the code illustrates, 729 node points were used which generated 4374 dynamic degrees of freedom for the excited

structure. Figure 3 depicts missile geometry as generated by the code upon building the model.

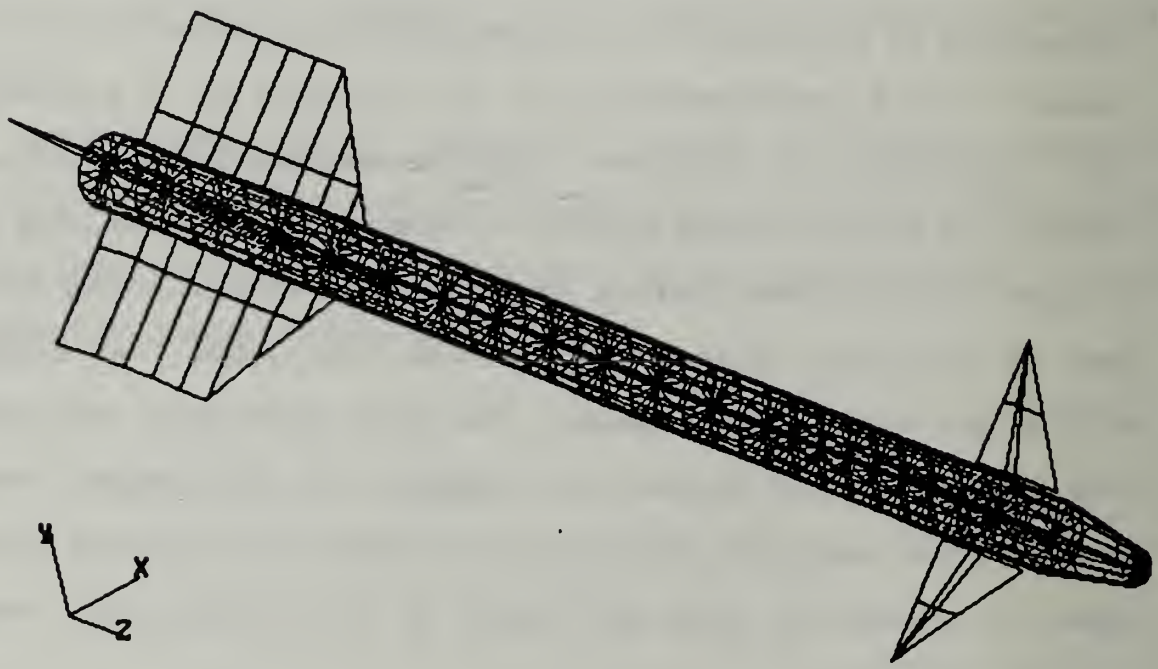

Refined Model Geometry

Figure 3

The large number of nodes was required to mathematically represent the missile. Instead of using curved beam segments which the software does not support, concentric rings consisting of 16 nodes joined with small quadrilateral plate elements were utilized to represent the missile cylindrical body. The concentric rings were spaced closely at three inches apart to avoid aspect ratios within the plate elements of greater than four to one, as the dynamic response becomes unreliable above this ratio. The resulting geometry yielded thirty five concentric rings of node points comprising the uniform cross section of the cylindrical body and three decreasing radius rings of node points comprising the tapering nose cone. Quadrilateral plate elements of .25 inch thickness were used in defining the skin of the cylinder and nose cone, while triangular plates of .25 inch thickness were used to describe the cone tip and the rear plate of the missile. The AIM-9 attaches to the LAU-7 launcher rail at three points. This was modeled by zeroing the displacements at points 85, 213 and 373 in the x,y and z directions as well as zeroing the rotations about the y and z axes. Rotation about the x axis was not zeroed since the motion in pitch is of primary interest here.

The front fins were constructed using a combination of quadrilateral and triangular plates each of 0.10 inch thickness. The AIM-9 front fins are actually moveable canards which rotate symmetrically about their attachment axis. Initially it was thought that this feature would pose an attachment problem to accurately represent the canards for dynamic analysis. This however did not

impact modeling. The concern of this investigation is primarily developing a methodology for predicting wing flutter induced by weapon/wing interaction. In order for flutter to take place the weapon must be attached to the wing and the missile maneuvering canards would be disabled. The canards were attached to the missile via a .035 inch plate. Due to the small size of the attachment plate the front fins exhibited an insufficient stiffness problem which could be addressed easily with further work on a subsequent model.

The rear wings were modeled using a combination of 0.5 inch quadrilateral and triangular plates. These were rigidly attached to the missile body using the laterally arrayed node points of successive concentric body rings.

The mass distribution node points represent the most significant refinement of the finite element model. Twenty-two mass distribution nodes were located along the geometric centerline of the missile. Each missile component (i.e. motor, seeker, warhead, etc.) received it's allotted number of nodes depending on its centerline axis dimension. These nodes were then secured spatially to the missile via a wagon wheel spoke arrangement which connected each mass node to the nodes located on the corresponding concentric cylindrical body ring. These connection elements were then assigned material properties according to what structure they were to materially represent (i.e. Propellent, explosive, seeker etc.). The mass for each missile component was then evenly distributed among the appropriate nodes. This arrangement provided the most accurate

representation of the actual missile structure and weight distribution.

C. MODE AND FREQUENCY CORRESPONDENCE

Completion of the model geometry enabled the pursuit of the next investigative goal, correspondence of the model generated modes and frequencies to those determined experimentally. In order to accomplish this, sequential static and dynamic response evaluations utilizing the "Build Model", "Statics" and "Dynamics" features of the software were required to assess the affect of the conformal adjustments made on the model. These adjustments were performed on a trial and error basis in order to achieve the highest degree of correspondence to the experimentally derived parameters. In using the "Build Model" feature the system stiffness, damping and mass matrices were formed. These were compiled based on Newton's Second Law of Motion which provides the foundation upon which all vibrational work is performed. Written as a second order differential equation in the time domain we obtain the following:

$$M*\ddot{z}_{(t)}+C*\dot{z}_{(t)}+K*z_{(t)}=f_{(t)} \tag{37}$$

Where

$$\begin{aligned} M &= \textit{system mass matrix} \\ C &= \textit{system damping matrix} \\ K &= \textit{system stiffness matrix} \\ x_{(t)} &= \textit{nodal displacement vector} \\ \dot{x}_{(t)} &= \textit{nodal velocity vector} \\ \ddot{x}_{(t)} &= \textit{nodal acceleration vector} \\ f_{(t)} &= \textit{applied force vector} \end{aligned} \tag{38}$$

The system equations formed during a modes analysis include the system stiffness and mass matrices, which when placed in matrix notation yields the following:

$$M*\ddot{x} + K*x = 0 \qquad (39)$$

This function is set to zero since there is no forcing function in normal modes analysis. All motion is assumed to be steady state harmonic motion. The missile oscillates at some frequency $f_{(i)}$, with each point moving either in or out of phase. Thus the node acceleration vector may be written in terms of the displacement vector as:

$$\ddot{x} = -(2*\pi*f)^2*x \qquad (40)$$

Substitution then yields:

$$[\ K - (2*\pi*f)^2*M\ ]*x \qquad (41)$$

Excluding the trivial solution, the remaining non-trivial solution to equation (39) produces the system of natural frequencies for the specific finite element model. Associated with each of these is a companion mode shape. As there is no forcing function utilized during the normal modes analysis, the scaling parameters are independently arbitrary so that only the relative mode shape holds any meaning.

The normal modes analysis in this study were accomplished utilizing the sub-space iteration feature on the software since only the lowest few resonant frequencies were sought. These were selected because in reality only the first few natural frequencies are excited to resonance by the dynamic forces applied to the system. Therefore these are of primary interest in predicting wing flutter. The sub-space iteration method solves for the eigenvectors and the eigenvalues utilizing the mass and stiffness matrices in equation (40). These matrices are derived from the material characteristics coded into the model. The results of the static and dynamic analysis using sub-space iteration on the finite element model are presented in Appendix A.

Evaluation of the refined models initial modal analysis revealed that the three lowest fundamental frequencies in pitch, which were the frequencies of interest for this study, were significantly different than the experimentally derived values. This indicated that the physical characteristic parameters within the model code required adjustment to more accurately represent the real missile. This was accomplished in increments. First, the modulus of the propellent was adjusted according to published data on propellent formulation and structuring criteria. This brought the frequencies into correct perspective relative to each other. The modulus of the warhead was changed next on a trial and error basis in an attempt to bring the frequencies into closer correspondence with the experimentally derived values. This effort was successful as evidenced by figure 4. This graphical

representation of the first three natural frequencies as each improvement to the finite element model was made, depicts the progressive honing of the model towards the physical reality of the actual missile. The experimentally obtained values are depicted by the white diamonds, and represent the first three natural modes of the AIM-9 Sidewinder. The first three modes as produced by the original finite element model are shown by the black squares with grey circle centers. As is evident by the graph, there is quite a disparity in the values, particularly in the second mode. With the addition of the centerline axis for mass distribution, as shown by the white squares with grey centers, we see a marked improvement in second mode correspondence with a degradation in first and third correspondence. As the propellent modulus was adjusted an improvement in first and second modes is noted with further degradation in the third mode. Here for the first time correct relative position between modes is noted. With the adjustment of the warhead modulus as represented by the grey diamonds, marked improvement in all three modes is seen for the closest correspondence to the experimental values. Further improvement in frequency correspondence could be obtained with continued refinement of the missile component physical characteristics. At the conclusion of this investigation model frequencies were within 6% for modes 1 and 3, and within 18% for mode 2. Table one illustrates the frequencies presented in Figure 4 as obtained in the progressive refinement of the finite element model.

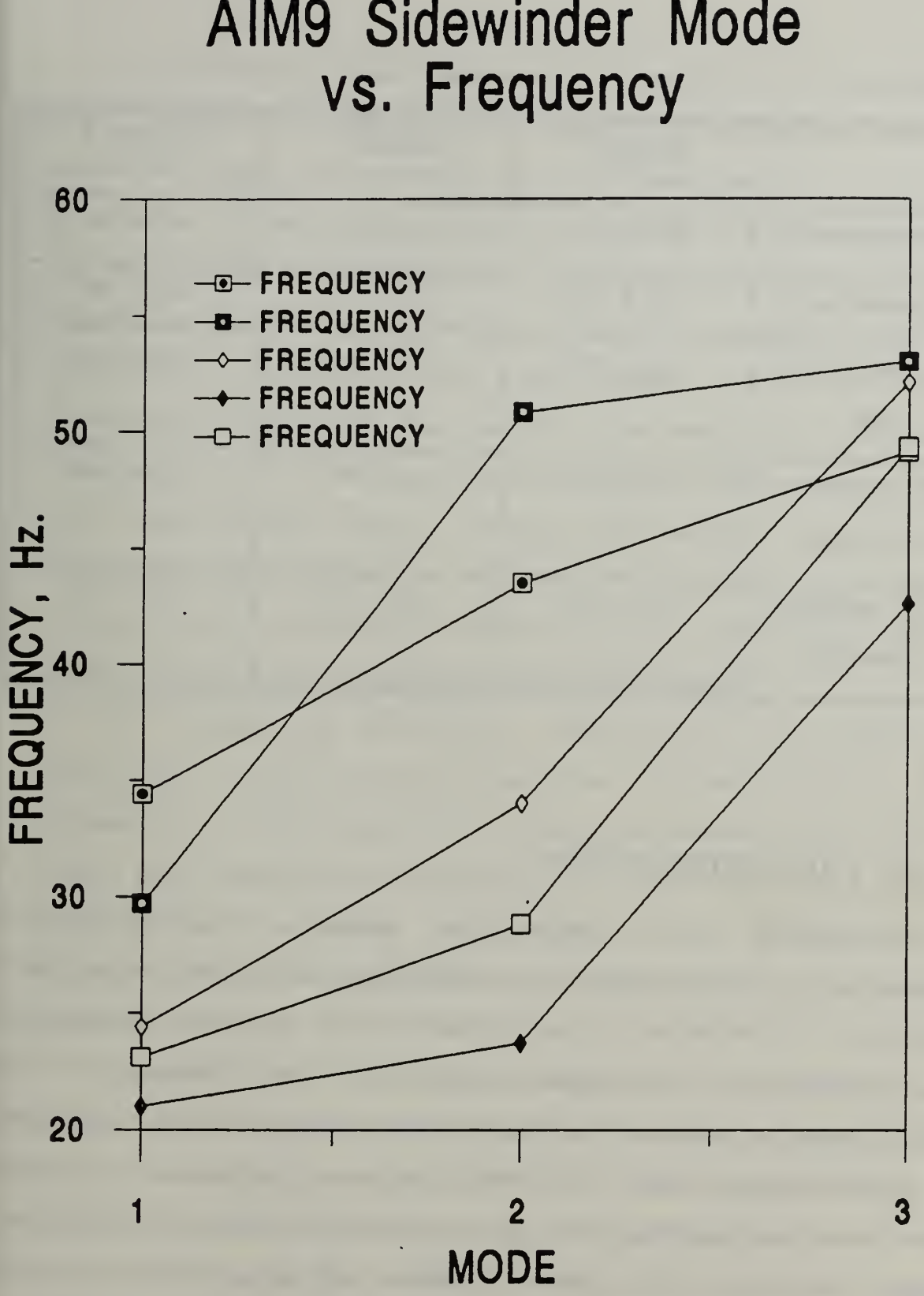
AIM9 Sidewinder Mode vs. Frequency
60
50
40
30
20
FREQUENCY, Hz.
FREQUENCY
FREQUENCY
FREQUENCY
FREQUENCY
FREQUENCY
1
2
3
MODE

Figure 4.

Table 1.

	MODE 1	MODE 2	MODE 3
ORIGINAL MODEL	29.7 Hz.	50.8 Hz	53.0 Hz
MEASURED DATA	24.4 Hz	34.0 Hz	52.1 Hz
1st CENTERLINE RUN	34.4 Hz	43.5 Hz	49.1 Hz
ADJ. PROPEL. MODULUS	21.0 Hz	23.6 Hz	42.7 Hz
ADJ. WARHEAD MODULUS	23.7 Hz	28.1 Hz	52.1 Hz

C. PARAMETRIC STUDY

Versatility and adaptability earmark a truly utile methodology. It was identified as desirable while developing this capability, to maintain to the greatest extent possible the ability to incorporate and accommodate physical block changes in the subject missile. Research and development will yield more efficient and durable propellants, warheads, guidance packages and seeker heads to be incorporated into future models of existing weapons or totally new kill stores. These changes must be accounted for to accurately predict wing-kill store interactive wing flutter.

To investigate this methodology's sensitivity to any physical block change in the subject weapon, a parametric study was conducted using the refined finite element model for the AIM-9 Sidewinder. Gross mass and modulus of elasticity changes were made for the warhead and rocket motor. These two missile components were chosen because they comprise the majority (upwards of 75%) of the missiles mass and length. With these changes, evaluations were made to determine the impact they had on 1. The modal characteristics of the missile, and 2. The systems calculation completion sensitivity (will the program crash). Finally, the missile casing material parameters were changed to represent a potential future composite casing. Again an evaluation was performed to determine the modal ramifications given composite casing replacement.

In varying the modulus of elasticity of the rocket motor propellent it was desired to examine the ramifications on mode frequency. In anticipation of future improvements in propellent yield, burn temperature and density only lower than present modulus examples were evaluated. Evaluations at 50% original and 25% original modulus were performed. The data results are presented in Appendix A.

The variation of the warhead weight was accomplished over the entire lineal length of the missile. As the anticipated weight saving advancements mentioned above are accomplished, more explosive may be added to the weapon to increase its effective kill radius. Thus the weight variation study took place over a range of 125% mass increase to 60% mass reduction in the warhead component.

The data results are presented in Appendix A. Simulation of a composite missile skin was desired in anticipation of its incorporation into the actual production weapon in the near future. This would engender both a significant weight savings on the order of 20%, and provide a strength and flexibility improvement which would translate directly into a missile performance enhancement. A currently available carbon fiber composite was utilized with the physical material data incorporated into the model by changing the material component parameters. The data results are presented in Appendix A. This simulation represents all of the quadrilateral plates comprising the missile skin as similar plates made of the chosen carbon fiber composite. All of the connection methods and geometric specifications remain the same.

III. CONCLUSIONS

In formulating this study it quickly became apparent that the tools necessary to thoroughly accomplish the development of an accurate wing to wing store interactive flutter prediction methodology were already in existence. The wing stores to be examined readily lent themselves structurally to finite element modeling and an increasingly accurate representation could be accomplished. The key to the more accurate solutions lay in understanding the software's capability to geometrically compose the various weapon components and the interrelationships these different components made in the formulation of the systems of equations which represented the physical dynamic response. As an example, the incorporation of the centerline mass distribution axis provided an increased capability to distribute the mass components of the model in a more refined manner. Thus an increased correspondence to the experimental data in the first three natural frequencies was accomplished. In the parametric study mass increases or decreases didn't affect the modes as much as where the mass was located spatially. This was evident in the differences seen between the original model, which had the masses placed on the skin of the model, and the refined centerline mass model which distributes the mass evenly along the geometric centerline. Accordingly, individual component modulus changes did not impact modes as did the relative positioning of different modulus values

along the missile length. A combination of mass, modulus and location /juxtaposition of these values could significantly impact model natural frequencies.

The techniques developed and described in this investigation are worthy of further work. The methodology accumulating throughout the three thesis' to date will ultimately result in the ability to accurately predict potential weapon/wing store interactive wing flutter for the price of a technicians time. This would save millions of taxpayer dollars.

IV. RECOMMENDATIONS

Further refinement of the finite element model is possible and required. Continued refinement of the fin attachment points to the missile body would further increase the realism of the mathematical representation. Stiffening of the existing attachments plus the addition of multiple adjacent attachments are potential solutions. The aft end plate also requires some modification. The actual missile incorporates a Con-Di nozzle especially engineered to maintain a constant burn rate over the firing life of the propellent. This must be simulated in replacement of the flat circular end plate now incorporated. This could be accomplished utilizing converging triangular plates into the aft end of the missile.

The GVT stand analysis hardware could also be upgraded and optimized. Replacing the current data accumulation and analysis equipment with a spectrum analyzer would enable the rapid experimental determination of the systems natural frequencies referenced to all axes of interest with a minimum of re-program and alternate hardware placement.

Further investigation of the GVT, launcher, rail interaction in all axes of interest would be required to determine the amount of interference (if any) being produced between the weapon and the wing. Stiffening of the GVT would also be required if the two other

primary axes of motion were to be investigated as yaw and roll axes signals are overcome with interference.

APPENDIX A

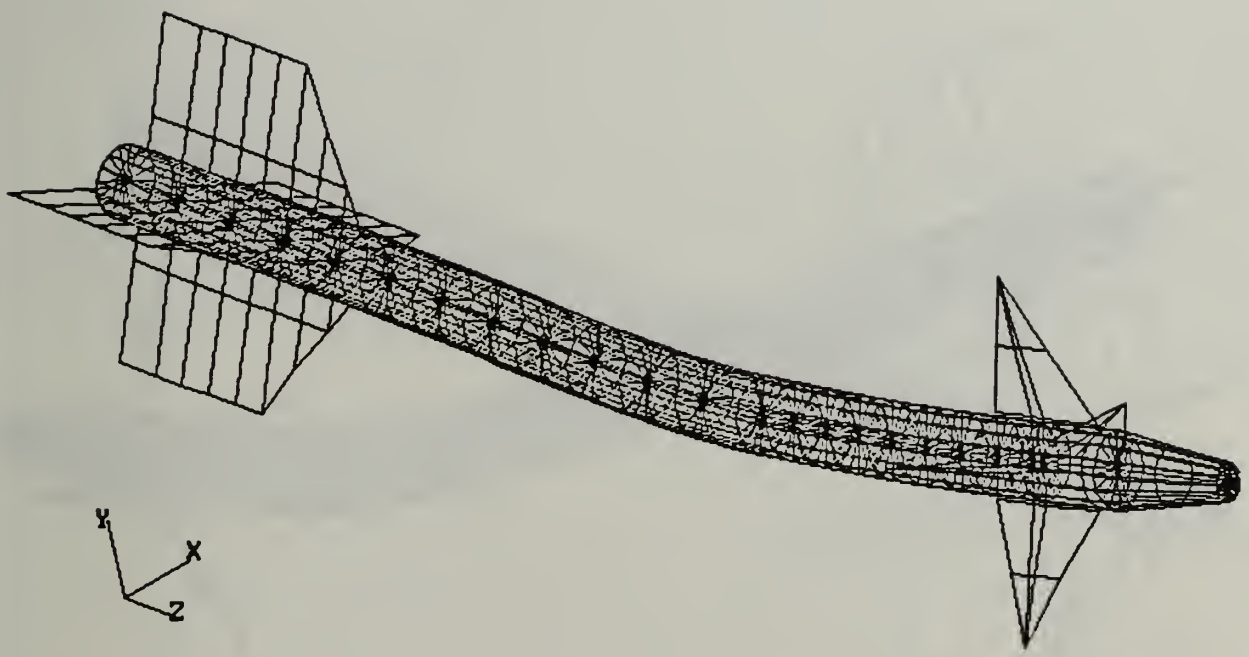

Mode 1

Figure 5.

MSC/pal 2

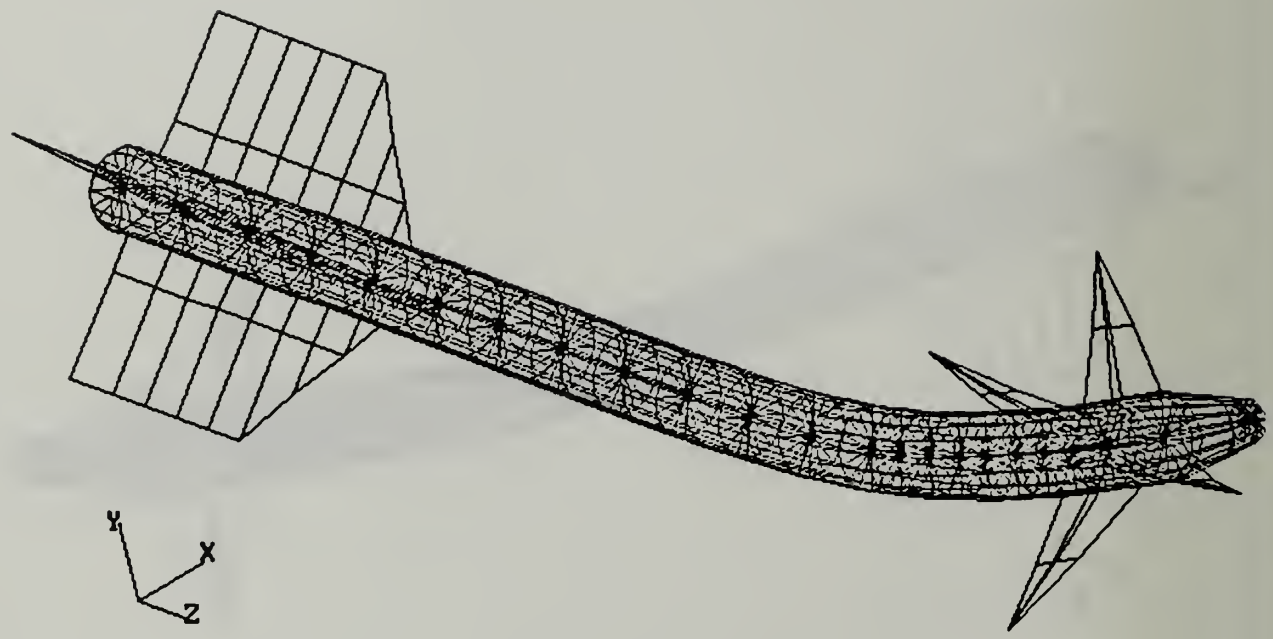

Mode 2

Figure 6.

MSC/pal 2

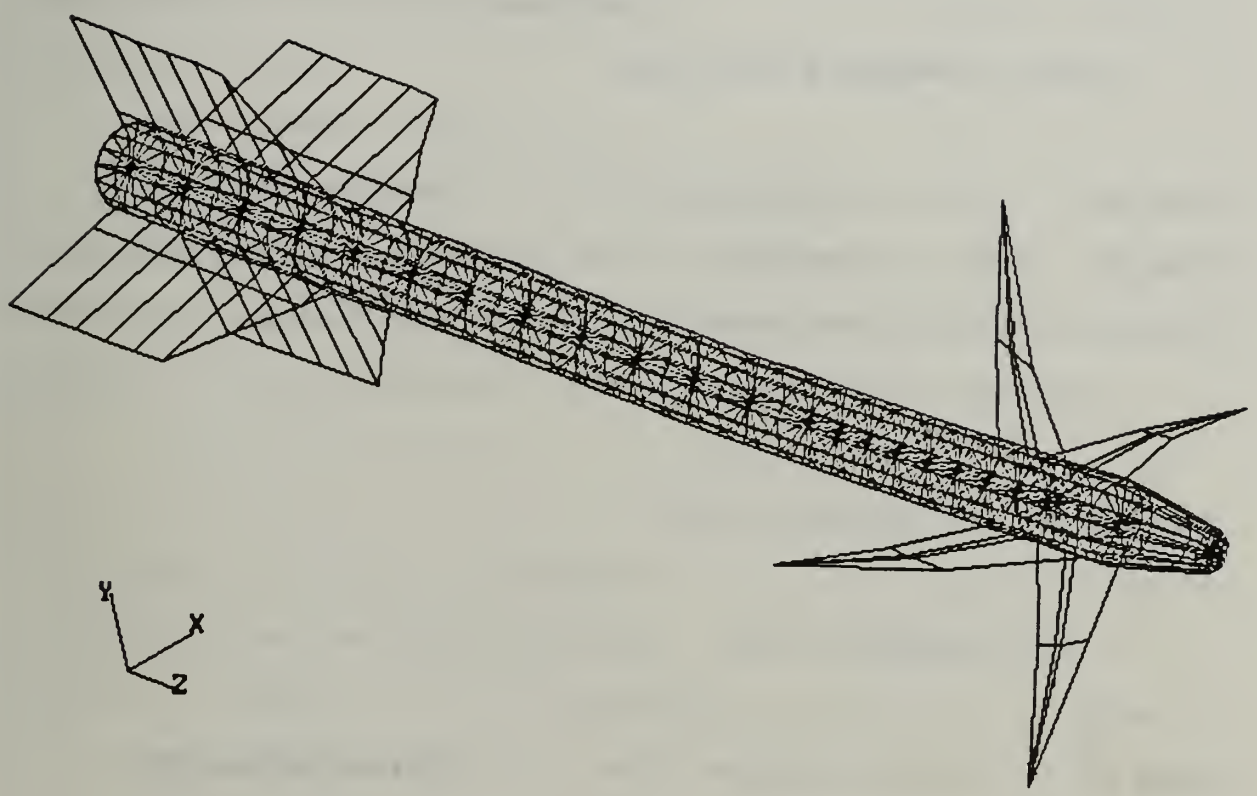

Mode 3

Figure 7.

MODE and FREQUENCY DATA

ORIGINAL WEIGHT DISTRIBUTION ON CENTERLINE AXIS

12-09-91 14:21 MSC/PAL 2 V 4.0 Page 1

- AIM9 GEOMETRY FILE

MODE NO. 1 AT 3.43604E+01 CPS (2.15893E+02 RAD/SEC)

MODE NO. 2 AT 4.35337E+01 CPS (2.73530E+02 RAD/SEC)

MODE NO. 3 AT 4.91267E+02 CPS (3.08672E+02 RAD/SEC)

MODULUS AT .25 ORIGINAL VALUE

12-11-91 11:23 MSC/PAL 2 V 4.0 Page 1

- AIM9 GEOMETRY FILE

MODE NO. 1 AT 2.10428E+01 CPS (1.32216E+02 RAD/SEC)

MODE NO. 2 AT 2.32971E+01 CPS (1.46380E+02 RAD/SEC)

MODE NO. 3 AT 4.24137E+01 CPS (2.66493E+02 RAD/SEC)

MODULUS AT .50 ORIGINAL VALUE

12-10-91 17:53 MSC/PAL 2 V 4.0 Page 1

-AIM9 GEOMETRY FILE

MODE NO. 1 AT 2.10642E+01 CPS (1.32350e+02 RAD/SEC)

MODE NO. 2 AT 2.33299E+01 CPS (1.46586E+02 RAD/SEC)

MODE NO. 3 AT 4.26267E+01 CPS (2.67831E+02 RAS/SEC)

WARHEAD MASS AT .50 ORIGINAL VALUE

12-12-91 11:11 MSC/PAL 2 V 4.0 Page 2

-AIM9 GEOMETRY FILE

MODE NO. 1 AT 2.10572E+01 CPS (1.32306E+02 RAD/SEC)

MODE NO. 2 AT 2.33381E+01 CPS (1.46638E+02 RAD/SEC)

MODE NO. 3 AT 4.26968E+01 CPS (2.698272E+02 RAD/SEC)

WARHEAD MASS AT .40 ORIGINAL VALUE

12-04-91 15:17 MSC/PAL 2 V 4.0 Page 2

-AIM9 GEOMETRY FILE

MODE NO. 1 AT 3.00438E+01 CPS (1.88771E+02 RAD/SEC)

MODE NO. 2 AT 5.09137E+01 CPS (3.19900E+02 RAD/SEC)

MODE NO. 3 AT 5.29758E+01 CPS (3.32857E+02 RAD/SEC)

WARHEAD MASS AT .60 ORIGINAL VALUE

12-04-91 17:15 MSC/PAL 2 V. 4.0 Page 2

-AIM9 GEOMETRY FILE

MODE NO. 1 AT 3.02458E+01 CPS (1.90040E+02 RAD/SEC)

MODE NO. 2 AT 5.09760E+01 CPS (3.20291E+02 RAD/SEC)

MODE NO. 3 AT 5.29784E+01 CPS (3.32873E+02 RAD/SEC)

WARHEAD MASS 1.25 ORIGINAL VALUE

12-11-91 18:34 MSC/PAL 2 V 4.0 Page 3

-AIM9 GEOMETRY FILE

MODE NO. 1 AT 2.10205E+01 CPS (1.32076E+02 RAD/SEC)

MODE NO. 2 AT 2.32820E+01 CPS (1.46285E+02 RAD/SEC)

MODE NO. 3 AT 4.23380E+01 CPS (2.66017E+02 RAD/SEC)

FINITE ELEMENT MODEL WITH TOTAL COMPOSITE CASE

12-19-91 18:06 MSC/PAL 2 V 4.0 Page 3

-AIM9 GEOMETRY FILE

MODE NO. 1 AT 1.98019E+01 CPS (1.24419E+02 RAD/SEC)

MODE NO. 2 AT 2.14401E+01 CPS (1.34712E+02 RAD/SEC)

MODE NO. 3 AT 3.90748E+02 CPS (2.45514E+02 RAD/SEC)

```
TITLE - AIM9 GEOMETRY FILE
C
C DEFINE NODES FOR MISSILE BODY
C
NODE 3
1 2.50, 0, 0 THROUGH 16 2.50, 337.5, 0
545 2.50, 0, 102 THROUGH 560 2.50, 337.5, 102
561 0, 0, 0

NODE 22
1, 16, 560, 1, 16

NODE 22
1, 16, 560, 15, 16

NODE 3
562 2.50, 0, 103 THROUGH 577 2.50, 337.5, 103
594 1.25, 0, 112 THROUGH 609 1.25, 337.5, 112

NODE 22
562, 577, 609, 1, 16

NODE 22
562, 577, 609, 15, 16

NODE 3
610 0, 0, 113

NODE 1
17 0,0,-1 THROUGH 32 0,0,-1

NODE 1
145 0, 0, -1 THROUGH 160 0, 0, -1

NODE 1
529 0, 0, -2 THROUGH 544 0, 0, -2

C Missile Centerline Mass Distribution Nodes

NODE 1
707 0,0,6
708 0,0,12
709 0,0,18
710 0,0,24
711 0,0,30
712 0,0,36
713 0,0,42
714 0,0,48
715 0,0,54
716 0,0,60
717 0,0,66
718 0,0,72
719 0,0,75
720 0,0,78
721 0,0,81
722 0,0,84
723 0,0,87
724 0,0,90
725 0,0,93
726 0,0,96
```

```
727 0,0,97
728 0,0,103
729 0,0,112

C DEFINE NODE POINTS FOR FRONT FINS

C
NODE 3
611 2.75, 45, 93
612 2.75, 45, 96
613 2.75, 45, 97
614 2.75, 45, 101.5
615 7.00, 45, 97.25
616 7.00, 45, 95
617 7.00, 45, 94.5
618 7.00, 45, 93
619 11.25, 45, 93
620 2.75, 135, 93
621 2.75, 135, 96
622 2.75, 135, 97
623 2.75, 135, 101.5
624 7.00, 135, 97.25
625 7.00, 135, 95
626 7.00, 135, 94.5
627 7.00, 135, 93
628 11.25, 135, 93
629 2.75, 225, 93
630 2.75, 225, 96
631 2.75, 225, 97
632 2.75, 225, 101.5
633 7.00, 225, 97.25
634 7.00, 225, 95
635 7.00, 225, 94.5
636 7.00, 225, 93
637 11.25, 225, 93
638 2.75, 315, 93
639 2.75, 315, 96
640 2.75, 315, 97
641 2.75, 315, 101.5
642 7.00, 315, 97.25
643 7.00, 315, 95
644 7.00, 315, 94.5
645 7.00, 315, 93
646 11.25, 315, 93

C
C DEFINE NODE POINTS FOR REAR WINGS
C
NODE 3
647 4.75, 45, 2
648 4.75, 45, 6
649 4.75, 45, 9
650 4.75, 45, 12
651 4.75, 45, 15
652 4.75, 45, 18
653 4.75, 45, 21
654 4.75, 45, 24
655 7.88, 45, 21
656 11.50, 45, 18
657 11.50, 45, 15
```

```
658 11.50, 45, 12
659 11.50, 45, 9
660 11.50, 45, 6
661 11.50, 45, 2
662 4.75, 135, 2
663 4.75, 135, 6
664 4.75, 135, 9
665 4.75, 135, 12
666 4.75, 135, 15
667 4.75, 135, 18
668 4.75, 135, 21
669 4.75, 135, 24
670 7.88, 135, 21
671 11.50, 135, 18
672 11.50, 135, 15
673 11.50, 135, 12
674 11.50, 135, 9
675 11.50, 135, 6
676 11.50, 135, 2
677 4.75, 225, 2
678 4.75, 225, 6
679 4.75, 225, 9
680 4.75, 225, 12
681 4.75, 225, 15
682 4.75, 225, 18
683 4.75, 225, 21
684 4.75, 225, 24
685 7.88, 225, 21
686 11.50, 225, 18
687 11.50, 225, 15
688 11.50, 225, 12
689 11.50, 225, 9
690 11.50, 225, 6
691 11.50, 225, 2
692 4.75, 315, 2
693 4.75, 315, 6
694 4.75, 315, 9
695 4.75, 315, 12
696 4.75, 315, 15
697 4.75, 315, 18
698 4.75, 315, 21
699 4.75, 315, 24
700 7.88, 315, 21
701 11.50, 315, 18
702 11.50, 315, 15
703 11.50, 315, 12
704 11.50, 315, 9
705 11.50, 315, 6
706 11.50, 315, 2

C
C ENTER MATERIAL PROPERTIES
C  YOUNGS  SHEAR  MASS DENS  POISSON  TENSILE STRENGTH
MAT 30.0E6, 12.0E6, 7.76E-4, 0.25, 30.0E3
C
C DEFINE PLATE TYPE FOR MISSILE BODY
C
QUAD 1, 1, 0.25
GENERATE CONNECTS 1, 16, 560, 1, 16
GENERATE CONNECTS 1, 16, 560, 15, 16
```

```
GENERATE CONNECTS 562, 577, 609, 1, 16
GENERATE CONNECTS 562, 577, 609, 15, 16
C
C DEFINE REAR MISSILE PLATE AND CONNECTIVITY
C
TRI 1, 2, 0.25
CON 1 TO 2 TO 561
CON 2 TO 3 TO 561
CON 3 TO 4 TO 561
CON 4 TO 5 TO 561
CON 5 TO 6 TO 561
CON 6 TO 7 TO 561
CON 7 TO 8 TO 561
CON 8 TO 9 TO 561
CON 9 TO 10 TO 561
CON 10 TO 11 TO 561
CON 11 TO 12 TO 561
CON 12 TO 13 TO 561
CON 13 TO 14 TO 561
CON 14 TO 15 TO 561
CON 15 TO 16 TO 561
CON 16 TO 1 TO 561
C
C DEFINE PLATE CAP CONNECTIVITY OF NOSE CONE
C
CON 594 TO 595 TO 610
CON 595 TO 596 TO 610
CON 596 TO 597 TO 610
CON 597 TO 598 TO 610
CON 598 TO 599 TO 610
CON 599 TO 600 TO 610
CON 600 TO 601 TO 610
CON 601 TO 602 TO 610
CON 602 TO 603 TO 610
CON 603 TO 604 TO 610
CON 604 TO 605 TO 610
CON 605 TO 606 TO 610
CON 606 TO 607 TO 610
CON 607 TO 608 TO 610
CON 608 TO 609 TO 610
CON 609 TO 594 TO 610
C
C CONNECT BODY TO NOSECONE
C
QUAD 1, 1, 0.25
CON 545 TO 562 TO 563 TO 546
CON 546 TO 563 TO 564 TO 547
CON 547 TO 564 TO 565 TO 548
CON 548 TO 565 TO 566 TO 549
CON 549 TO 566 TO 567 TO 550
CON 550 TO 567 TO 568 TO 551
CON 551 TO 568 TO 569 TO 552
CON 552 TO 569 TO 570 TO 553
CON 553 TO 570 TO 571 TO 554
CON 554 TO 571 TO 572 TO 555
CON 555 TO 572 TO 573 TO 556
CON 556 TO 573 TO 574 TO 557
CON 557 TO 574 TO 575 TO 558
CON 558 TO 575 TO 576 TO 559
CON 559 TO 576 TO 577 TO 560
```

```
CON 560 TO 577 TO 562 TO 545

MAT 30.0E6, 12.0E6, 7.76E-5, 0.25, 30.0E3

BEAM 3, 0.5, 0.25
C
C CONNECTING CENTERLINE NODES TO EACH OTHER AND TO SURFACE NODES
CON 561 TO 707
C
CON 707 TO 708
CON 708 TO 709
CON 709 TO 710
CON 710 TO 711
CON 711 TO 712
CON 712 TO 713
CON 713 TO 714
CON 714 TO 715
CON 715 TO 716
CON 716 TO 717
CON 717 TO 718
CON 718 TO 719
CON 719 TO 720
CON 720 TO 721
CON 721 TO 722
CON 722 TO 723
CON 723 TO 724
CON 724 TO 725
CON 725 TO 726
CON 726 TO 727
CON 727 TO 728
CON 728 TO 729
CON 729 TO 610
CON 707 TO 33
CON 707 TO 34
CON 707 TO 35
CON 707 TO 36
CON 707 TO 37
CON 707 TO 38
CON 707 TO 39
CON 707 TO 40
CON 707 TO 41
CON 707 TO 42
CON 707 TO 43
CON 707 TO 44
CON 707 TO 45
CON 707 TO 46
CON 707 TO47
CON 707 TO 48
CON 708 TO 65
CON 708 TO 66
CON 708 TO 67
CON 708 TO 68
CON 708 TO 69
CON 708 TO 70
CON 708 TO 71
CON 708 TO 72
CON 708 TO 73
CON 708 TO 74
CON 708 TO 75
CON 708 TO 76
```

```
CON 708 TO 77
CON 708 TO 78
CON 708 TO 79
CON 708 TO 80
CON 709 TO 97
CON 709 TO 98
CON 709 TO 99
CON 709 TO 100
CON 709 TO 101
CON 709 TO 102
CON 709 TO 103
CON 709 TO 104
CON 709 TO 105
CON 709 TO 106
CON 709 TO 107
CON 709 TO 108
CON 709 TO 109
CON 709 TO 110
CON 709 TO 111
CON 709 TO 112
CON 710 TO 129
CON 710 TO 130
CON 710 TO 131
CON 710 TO 132
CON 710 TO 133
CON 710 TO 134
CON 710 TO 135
CON 710 TO 136
CON 710 TO 137
CON 710 TO 138
CON 710 TO 139
CON 710 TO 140
CON 710 TO 141
CON 710 TO 142
CON 710 TO 143
CON 710 TO 144
CON 711 TO 161
CON 711 TO 162
CON 711 TO 163
CON 711 TO 164
CON 711 TO 165
CON 711 TO 166
CON 711 TO 167
CON 711 TO 168
CON 711 TO 169
CON 711 TO 170
CON 711 TO 171
CON 711 TO 172
CON 711 TO 173
CON 711 TO 174
CON 711 TO 175
CON 711 TO 176
CON 712 TO 194
CON 712 TO 195
CON 712 TO 196
CON 712 TO 197
CON 712 TO 198
CON 712 TO 199
CON 712 TO 200
CON 712 TO 201
```

```
CON 712 TO 202
CON 712 TO 203
CON 712 TO 204
CON 712 TO 205
CON 712 TO 206
CON 712 TO 206
CON 712 TO 207
CON 712 TO 208
CON 713 TO 225
CON 713 TO 226
CON 713 TO 227
CON 713 TO 228
CON 713 TO 229
CON 713 TO 230
CON 713 TO 231
CON 713 TO 232
CON 713 TO 233
CON 713 TO 234
CON 713 TO 235
CON 713 TO 236
CON 713 TO 237
CON 713 TO 238
CON 713 TO 239
CON 713 TO 240
CON 714 TO 257
CON 714 TO 258
CON 714 TO 259
CON 714 TO 260
CON 714 TO 261
CON 714 TO 262
CON 714 TO 263
CON 714 TO 264
CON 714 TO 265
CON 714 TO 266
CON 714 TO 267
CON 714 TO 268
CON 714 TO 269
CON 714 TO 270
CON 714 TO 271
CON 714 TO 272
CON 715 TO 289
CON 715 TO 290
CON 715 TO 291
CON 715 TO 292
CON 715 TO 293
CON 715 TO 294
CON 715 TO 295
CON 715 TO 296
CON 715 TO 297
CON 715 TO 298
CON 715 TO 299
CON 715 TO 300
CON 715 TO 301
CON 715 TO 302
CON 715 TO 303
CON 715 TO 304
CON 716 TO 321
CON 716 TO 322
CON 716 TO 323
CON 716 TO 324
```

```
CON 716 TO 325
CON 716 TO 326
CON 716 TO 327
CON 716 TO 328
CON 716 TO 329
CON 716 TO 330
CON 716 TO 331
CON 716 TO 332
CON 716 TO 333
CON 716 TO 334
CON 716 TO 335
CON 716 TO 336
CON 717 TO 353
CON 717 TO 354
CON 717 TO 355
CON 717 TO 356
CON 717 TO 357
CON 717 TO 358
CON 717 TO 359
CON 717 TO 360
CON 717 TO 361
CON 717 TO 362
CON 717 TO 363
CON 717 TO 364
CON 717 TO 365
CON 717 TO 366
CON 717 TO 367
CON 717 TO 368

MAT 30.0E6, 12.0E6, 7.76E-4, 0.25, 30.0E3

CON 718 TO 385
CON 718 TO 386
CON 718 TO 387
CON 718 TO 388
CON 718 TO 389
CON 718 TO 390
CON 718 TO 391
CON 718 TO 392
CON 718 TO 393
CON 718 TO 394
CON 718 TO 395
CON 718 TO 396
CON 718 TO 397
CON 718 TO 398
CON 718 TO 399
CON 718 TO 400
CON 719 TO 401
CON 719 TO 402
CON 719 TO 403
CON 719 TO 404
CON 719 TO 405
CON 719 TO 406
CON 719 TO 407
CON 719 TO 408
CON 719 TO 409
CON 719 TO 410
CON 719 TO 411
CON 719 TO 412
CON 719 TO 413
```

```
CON 719 TO 414
CON 719 TO 415
CON 719 TO 416
CON 720 TO 418
CON 720 TO 419
CON 720 TO 420
CON 720 TO 421
CON 720 TO 422
CON 720 TO 423
CON 720 TO 424
CON 720 TO 425
CON 720 TO 426
CON 720 TO 427
CON 720 TO 428
CON 720 TO 429
CON 720 TO 430
CON 720 TO 431
CON 720 TO 432
CON 721 TO 433
CON 721 TO 434
CON 721 TO 435
CON 721 TO 436
CON 721 TO 437
CON 721 TO 438
CON 721 TO 439
CON 721 TO 440
CON 721 TO 441
CON 721 TO 442
CON 721 TO 443
CON 721 TO 444
CON 721 TO 445
CON 721 TO 446
CON 721 TO 447
CON 721 TO 448
CON 722 TO 449
CON 722 TO 450
CON 722 TO 451
CON 722 TO 452
CON 722 TO 453
CON 722 TO 454
CON 722 TO 455
CON 722 TO 456
CON 722 TO 457
CON 722 TO 458
CON 722 TO 459
CON 722 TO 460
CON 722 TO 461
CON 722 TO 462
CON 722 TO 463
CON 722 TO 464
CON 723 TO 465
CON 723 TO 466
CON 723 TO 467
CON 723 TO 468
CON 723 TO 469
CON 723 TO 470
CON 723 TO 471
CON 723 TO 472
CON 723 TO 473
CON 723 TO 474
```

```
CON 723 TO 475
CON 723 TO 476
CON 723 TO 477
CON 723 TO 478
CON 723 TO 479
CON 723 TO 480
CON 724 TO 482
CON 724 TO 483
CON 724 TO 484
CON 724 TO 485
CON 724 TO 486
CON 724 TO 487
CON 724 TO 488
CON 724 TO 489
CON 724 TO 490
CON 724 TO 491
CON 724 TO 492
CON 724 TO 493
CON 724 TO 494
CON 724 TO 495
CON 724 TO 496
CON 725 TO 497
CON 725 TO 498
CON 725 TO 499
CON 725 TO 500
CON 725 TO 501
CON 725 TO 502
CON 725 TO 503
CON 725 TO 504
CON 725 TO 505
CON 725 TO 506
CON 725 TO 507
CON 725 TO 508
CON 725 TO 509
CON 725 TO 510
CON 725 TO 511
CON 725 TO 512
CON 726 TO 513
CON 726 TO 514
CON 726 TO 515
CON 726 TO 516
CON 726 TO 517
CON 726 TO 518
CON 726 TO 519
CON 726 TO 520
CON 726 TO 521
CON 726 TO 522
CON 726 TO 523
CON 726 TO 524
CON 726 TO 525
CON 726 TO 526
CON 726 TO 527
CON 726 TO 528
CON 727 TO 529
CON 727 TO 530
CON 727 TO 531
CON 727 TO 532
CON 727 TO 533
CON 727 TO 534
CON 727 TO 535
```

```
CON 727 TO 536
CON 727 TO 537
CON 727 TO 538
CON 727 TO 539
CON 727 TO 540
CON 727 TO 541
CON 727 TO 542
CON 727 TO 543
CON 727 TO 544
CON 728 TO 545
CON 728 TO 546
CON 728 TO 562
CON 728 TO 563
CON 728 TO 564
CON 728 TO 565
CON 728 TO 566
CON 728 TO 567
CON 728 TO 568
CON 728 TO 569
CON 728 TO 570
CON 728 TO 571
CON 728 TO 572
CON 728 TO 573
CON 728 TO 574
CON 728 TO 575
CON 729 TO 594
CON 729 TO 595
CON 729 TO 596
CON 729 TO 597
CON 729 TO 598
CON 729 TO 599
CON 729 TO 600
CON 729 TO 601
CON 729 TO 602
CON 729 TO 603
CON 729 TO 604
CON 729 TO 605
CON 729 TO 606
CON 729 TO 607
CON 729 TO 608
CON 729 TO 609
C
MAT 30.0E6, 12.0E6, 7.76E-4, .25, 30.0E3

C FIRST FRONT FIN
C
QUAD 1, 1, 0.35
CON 515 TO 531 TO 613 TO 612
QUAD 1, 1, 0.10
CON 611 TO 612 TO 617 TO 618
CON 612 TO 613 TO 616 TO 617
CON 613 TO 614 TO 615 TO 616
TRI 1, 2, 0.10
CON 619 TO 618 TO 617
CON 619 TO 617 TO 616
CON 619 TO 616 TO 615
C
C SECOND FRONT FIN
C
QUAD 1, 1, 0.35
```

```
CON 519 TO 535 TO 622 TO 621
QUAD 1, 1, 0.1
CON 620 TO 621 TO 626 TO 627
CON 621 TO 622 TO 625 TO 626
CON 622 TO 623 TO 624 TO 625
TRI 1, 2, 0.1
CON 628 TO 627 TO 626
CON 628 TO 626 TO 625
CON 628 TO 625 TO 624
C
C THIRD FRONT FIN
C
QUAD 1, 1, 0.35
CON 523 TO 539 TO 631 TO 630
QUAD 1, 1, 0.1
CON 629 TO 630 TO 635 TO 636
CON 630 TO 631 TO 634 TO 635
CON 631 TO 632 TO 633 TO 634
TRI 1, 2, 0.1
CON 637 TO 636 TO 635
CON 637 TO 635 TO 634
CON 637 TO 634 TO 633
C
C FOURTH FRONT FIN
C
QUAD 1, 1, 0.35
CON 527 TO 543 TO 640 TO 639
QUAD 1, 1, 0.1
CON 638 TO 639 TO 644 TO 645
CON 639 TO 640 TO 643 TO 644
CON 640 TO 641 TO 642 TO 643
TRI 1, 2, 0.1
CON 646 TO 645 TO 644
CON 646 TO 644 TO 643
CON 646 TO 643 TO 642
C
C DEFINE REAR WING MATERIAL PROPERTIES
C
MAT 10E6, 4E6, 2.59E-4, 0.25, 10E3
C
C DEFINE REAR WING PLATE TYPE AND CONNECTIVITY
C
C FIRST REAR WING
C
QUAD 1, 1, 0.5
CON 19 TO 35 TO 648 TO 647
CON 647 TO 648 TO 660 TO 661
CON 35 TO 51 TO 649 TO 648
CON 648 TO 649 TO 659 TO 660
CON 51 TO 67 TO 650 TO 649
CON 649 TO 650 TO 658 TO 659
CON 67 TO 83 TO 651 TO 650
CON 650 TO 651 TO 657 TO 658
CON 83 TO 99 TO 652 TO 651
CON 651 TO 652 TO 656 TO 657
CON 99 TO 115 TO 653 TO 652
CON 652 TO 653 TO 655 TO 656
CON 115 TO 131 TO 654 TO 653
TRI 1, 2, 0.5
CON 654 TO 131 TO 147
```

```
CON 655 TO 653 TO 654
C
C SECOND REAR WING
C
QUAD 1, 1, 0.5
CON 23 TO 39 TO 663 TO 662
CON 662 TO 663 TO 675 TO 676
CON 39 TO 55 TO 664 TO 663
CON 663 TO 664 TO 674 TO 675
CON 55 TO 71 TO 665 TO 664
CON 664 TO 665 TO 673 TO 674
CON 71 TO 87 TO 666 TO 665
CON 665 TO 666 TO 672 TO 673
CON 87 TO 103 TO 667 TO 666
CON 666 TO 667 TO 671 TO 672
CON 103 TO 119 TO 668 TO 667
CON 667 TO 668 TO 670 TO 671
CON 119 TO 135 TO 669 TO 668
TRI 1, 2, 0.5
CON 669 TO 135 TO 151
CON 670 TO 668 TO 669
C
C THIRD REAR WING
C
QUAD 1, 1, 0.5
CON 27 TO 43 TO 678 TO 677
CON 677 TO 678 TO 690 TO 691
CON 43 TO 59 TO 679 TO 678
CON 678 TO 679 TO 689 TO 690
CON 59 TO 75 TO 680 TO 679
CON 679 TO 680 TO 688 TO 689
CON 75 TO 91 TO 681 TO 680
CON 680 TO 681 TO 687 TO 688
CON 91 TO 107 TO 682 TO 681
CON 681 TO 682 TO 686 TO 687
CON 107 TO 123 TO 683 TO 682
CON 682 TO 683 TO 685 TO 686
CON 123 TO 139 TO 684 TO 683
TRI 1, 2, 0.5
CON 684 TO 139 TO 155
CON 685 TO 683 TO 684
C
C FOURTH REAR WING
C
QUAD 1, 1, 0.5
CON 31 TO 47 TO 693 TO 692
CON 692 TO 693 TO 705 TO 706
CON 47 TO 63 TO 694 TO 693
CON 693 TO 694 TO 704 TO 705
CON 63 TO 79 TO 695 TO 694
CON 694 TO 695 TO 703 TO 704
CON 79 TO 95 TO 696 TO 695
CON 695 TO 696 TO 702 TO 703
CON 95 TO 111 TO 697 TO 696
CON 696 TO 697 TO 701 TO 702
CON 111 TO 127 TO 698 TO 697
CON 697 TO 698 TO 700 TO 701
CON 127 TO 143 TO 699 TO 698
TRI 1, 2, 0.5
CON 699 TO 143 TO 159
```

```
CON 700 TO 698 TO 699
C
C DEFINE ATTACHMENT POINTS OF MISSILE TO LAUNCHER
C
ZERO 1
TA 85, 213, 373
RY 85, 213, 373
RZ 85, 213, 373

C
C DEFINE LUMPED MASSES FOR SEPARATE MISSILE COMPONENTS
C
C  MASS DISTRIBUTION OF THE MOTOR
MASS 707, 0.02387
MASS 708, 0.02387
MASS 709, 0.02387
MASS 710, 0.02387
MASS 711, 0.02387
MASS 712, 0.02387
MASS 712, 0.02387
MASS 713, 0.02387
MASS 714, 0.02387
MASS 715, 0.02387
MASS 716, 0.02387
MASS 717, 0.02387

C  MASS DISTRIBUTION OF THE WARHEAD
MASS 718, 0.02133
MASS 719, 0.02133
MASS 720, 0.02133
MASS 721, 0.02133
MASS 722, 0.02133
MASS 723, 0.02133

C  MASS DISTRIBUTION OF THE GUIDANCE AND CONTROL
MASS 724, 0.00583
MASS 725, 0.00583
MASS 726, 0.00583
MASS 727, 0.00583
C  MASS DISTRIBUTION OF THE DETECTOR
MASS 728, 0.03365
MASS 729, 0.03365
END
```

BIBLIOGRAPHY

1. Hollyer, J. B., Ground Vibration characterization of a Missile System for Flutter Energy Definition, Masters Thesis, Naval Postgraduate School, Monterey California, June 1990.

2. Shutty, M. J., Dynamic Modeling and Modal Analysis of an Air-to-Air Missile, Masters Thesis, Naval Postgraduate School, Monterey California, September 1991.

3. Structural Measurement Systems, Basic Modal Testing and Analysis Techniques, 1991.

4. Entek Scientific Corporation, EMODAL-PC Learning Guide, 1988.

5. Scientific Atlanta, SD-380 Signal Analyzer Operators Manual.

6. Spectral Institute, Modal Analysis Training Course And Application Notes.

7. MacNeal-Schwendler Corp., MSC/PAL2 Advanced Stress and Vibration Analysis Version 4.0 Reference Manual, 1990.

8. MacNeal-Schwendler Corp., MSC/PAL2 Advanced Stress and Vibration Analysis Version 4.0 Users Manual, 1990.

9. Structural Measurement Systems, Basic Modal Testing and Analysis Techniques, 1991.

10. Thompson, W.T., Vibration Theory and Applications, Prentice-Hall ,Inc., 1965.

11. Friedland, B., Control System Design, An Introduction to State Space Methods, McGraw-Hill Co.

INITIAL DISTRIBUTION LIST

1. Library, Code 52 — 2
   Naval Postgraduate School
   Monterey, CA 93943-5002

2. Defense Technical Information Center — 2
   Cameron Station
   Alexandria, VA 22304-6145

3. Department Chairman, Code AA — 2
   Department of Aeronautics and Astronautics
   Naval Postgraduate School
   Monterey, CA 93943-5002

4. Flight Deck Officer CV-60 — 5
   ATTN. Lt. G.G. Van Dyke
   USS Saratoga, CV-60
   V-1 Division
   FPO AA34078-2740

5. Professor Edward Wu, Code AA/WU — 2
   Department of Aeronautics and Astronautics
   Naval Postgraduate School
   Monterey, CA 93943-5000